Optimum and Green Fabrication of MIL-100(Fe) for Crystal Violet Dye Removal from Aqueous Solution

Christian Julius Wijaya[1,2*], Felycia Edi Soetaredjo[1,2], Maria Yuliana[1,2], Shella Permatasari Santoso[1,2], Sandy Budi Hartono[1,2], Wenny Irawaty[1,2], Jenni Lie[1,2], Jindrayani Nyoo Putro[1,2], Chintya Gunarto[1,2], Nathania Puspitasari[1,2], Suryadi Ismadji[1,2], and Setiyo Gunawan[3]

[1]*Department of Chemical Engineering, Widya Mandala Surabaya Catholic University, Kalijudan 37, Surabaya 60114, Indonesia*

[2]*Collaborative Research Center for Zero Waste and Sustainability, Kalijudan 37, Surabaya 60114, Indonesia*

[3]*Department of Chemical Engineering, Faculty of Industrial Technology and Systems Engineering, Institut Teknologi Sepuluh Nopember, Keputih Sukolilo, Surabaya 60111, Indonesia*

* ***Corresponding author:***

email: christian_wijaya@ukwms.ac.id

Received: January 18, 2024
Accepted: June 3, 2024

DOI: 10.22146/ijc.93323

Abstract: *MIL-100(Fe) was prepared and subsequently used to remove crystal violet dye from aqueous solutions simulating dye-containing wastewater in the environment. In the future, it is aimed that MIL-100(Fe) can be used in managing dye-containing wastewater in the environment and reducing the negative impacts it can cause. Here, MIL-100(Fe) fabrication needs to be optimized to obtain optimum process conditions, which are environmentally friendly and can produce MIL-100(Fe) with the best characteristics. This study focused on optimizing the fabrication of MIL-100(Fe), which is a type of MOF with good chemical stability, thermal stability, and flexible structure. In this study, the room-temperature fabrication of MIL-100(Fe) was established using a ligand-to-metal molar ratio of 0.95 and an acetic acid concentration of 5.1 vol% for 6.2 h. The optimum MIL-100(Fe) was tested for crystal violet removal and provided an optimum removal capacity of 182.66 ± 3.81 mg/g. Statistical approaches are used to investigate the independent parameters and their interactions contributing to MIL-100(Fe) formation.*

Keywords: *crystal violet dye; metal-organic frameworks; MIL-100(Fe); optimization; statistical approach*

■ INTRODUCTION

Synthetic dyes are an important component in the textile industry and they are required in large quantities and variations. Around 10 thousand tons per year of synthetic dyes are needed in the worldwide textile industry [1]. Most of these dyes will be carried away in wastewater from the textile industry, where the concentration varies from 5 to 1,500 mg/L [2]. These dye contaminants in aquatic ecosystems are dangerous for the environment and public health due to their toxic functional groups, such as aromatic groups, amines, and metal contents [3]. Moreover, dyes are not only used in the textile industry but also in paper and pulp, foods, beverages, pharmaceuticals, cosmetics, and automotive industries.

The biggest challenge in handling this problem is that dyes generally have high solubility in water, so they are more challenging to be separated. Several technologies have been developed to treat dye-containing wastewater, such as membrane techniques, adsorption, advanced oxidation processes, bio-electrochemical treatments, and photocatalytic degradation [4-5]. Adsorption is a widely used technique because of its simplicity, ease of handling, low cost, high adsorption capacity, high efficiency, and less toxic by-products [3]. In the adsorption process, the adsorbent plays an essential role, so it needs to be selected by considering the type of dyes, wastewater conditions, adsorption effectiveness, and solid waste handling.

Iron-based materials of Institute Lavoisier-100 (MIL-100(Fe)), a type of metal-organic framework (MOFs), is a potential adsorbent for dye-containing wastewater. MIL-100(Fe) has high porosity, large pore volume [6], higher water stability [7-8], tailorable structure [9], and photocatalytic behavior [10]. However, conventional MIL-100(Fe) is still synthesized at high temperatures with the addition of corrosive acids, such as hydrofluoric acid and nitric acid [11]. Currently, novel MIL-100(Fe) synthesis techniques have been developed to obtain less hazardous methods using lower temperatures and less harmful solvents.

In this study, the fabrication of MIL-100(Fe) using environmentally friendly solvents under room-temperature conditions was developed and optimized to obtain the optimum MIL-100(Fe) with high removal capacity of crystal violet dye. In this study, crystal violet dye was used as a model simulating the dye-containing wastewater in the environment. Crystal violet dye itself is one of the common dyes used in the textile industry and discharged into the environment in wastewater. Statistical approaches were conducted to investigate the effects of three independent parameters: ligand-to-metal molar ratio, fabrication time, and acetic acid concentration. Further, the optimum fabricated MIL-100(Fe) was characterized to investigate the physical and chemical characteristics.

■ EXPERIMENTAL SECTION

Materials

Iron(III) nitrate nonahydrate ($Fe(NO_3)_3{\cdot}9H_2O$, 99 wt.%), benzene-1,3,5-tricarboxylic acid (H_3BTC, 95 wt.%), acetic acid (CH_3COOH, 99.7 wt.%), ethanol (C_2H_5OH, 99.9 wt.%), and crystal violet dye ($C_{25}N_3H_{30}Cl$, 90 wt.%) were purchased from Sigma-Aldrich (Singapore). All chemicals were of analytical grade and used as received.

Instrumentation

MIL-100(Fe) was characterized using X-ray diffraction (XRD), scanning electron microscopy (SEM), Fourier transform infrared spectroscopy (FTIR), thermalgravimetric analysis (TGA), and nitrogen (N_2) sorption to investigate its physical and chemical characteristics. XRD analysis was conducted by a PANalytical X'Pert Pro X-ray diffractometer with Cu $K\alpha_1$ radiation ($\lambda = 1.5406$ Å) at 40 kV and 30 mA to figure out the X-ray diffraction of MIL-100(Fe). SEM analysis was done by a JSM-6390 field emission SEM at 10 kV to map the morphology of MIL-100(Fe). FTIR analysis was performed by an FTIR Shimadzu 8400S with the KBr pelleting method to figure out the FTIR spectrum of MIL-100(Fe). TGA analysis was carried out by a Perkin Elmer Diamond TG/DTA thermal analyzer at a constant heating and cooling rate to figure the TGA and DTG spectra of MIL-100(Fe). N_2 sorption analysis was conducted at 77 K using a Micromeritics ASAP 2010 sorption analyzer after degassing the sample at 200 °C for 6 h.

Procedure

Fabrication of MIL-100(Fe)

MIL-100(Fe) was fabricated under room-temperature conditions using $Fe(NO_3)_3{\cdot}9H_2O$ as the metal source and H_3BTC as the ligand. Here, two solutions were prepared separately by dissolving $Fe(NO_3)_3{\cdot}9H_2O$ in 40 mL of aqueous acetic acid solution and H_3BTC in 40 mL of equimolar aqueous ethanol solution. Both solutions were sonicated for 10 min until completely dissolved. After that, the ligand solution was added dropwise into the metal solution and stirred at room temperature while red-brown solids were formed. Then, the solids were separated by centrifuge, washed using ethanol twice, and dried overnight at 70 °C utilizing an oven. The MIL-100(Fe) solids were then characterized and used for further applications.

Statistical and optimization studies

Three independent parameters were studied to determine their effects on the fabricated MIL-100(Fe), such as ligand-to-metal molar ratio (A), fabrication time (B), and acetic acid concentration (C). Here, the one-factor-at-a-time (OFAT) method was used to investigate this study, using the removal capacity of crystal violet as a response to this statistical study. Table 1 shows the parameters and their levels selected in this study as well as the basis for determining levels in the optimization study.

Table 1. The parameters and their levels for OFAT study

Parameters	Levels			
A	0.50	0.75	1.00	1.25
B (h)	2.0	4.0	6.0	8.0
C (vol%)	1.0	2.5	5.0	7.5

Table 2. The levels of each independent parameter for RSM study

Parameters	Levels				
	−1.68	−1	0	+1	+1.68
A	0.58	0.75	1.00	1.25	1.42
B (h)	2.6	4.0	6.0	8.0	9.4
C (vol%)	0.8	2.5	5.0	7.5	9.2

Furthermore, response surface methodology (RSM) was used to advance statistical studies with central composite design (CCD) as the experimental design using Minitab 19 statistical software. The same three independent parameters were used to investigate the linear, quadratic, and two-way effects on the fabricated MIL-100(Fe) with five levels for each parameter coded as –1.68, –1, 0, +1, and +1.68. Here, analysis of variance (ANOVA) was included in this RSM statistical study to investigate the significance of each parameter and combined parameter. In this CCD experimental design, there were three independent parameters with three levels and two extreme levels, each of which is shown in Table 2. Here, there were 60 runs of 20 runs per set with 3 replications.

The optimization study was also carried out in cooperation with the RSM study using the same data and statistical software. This study aimed to determine the optimum fabrication condition of MIL-100(Fe) with the highest removal capacity of crystal violet. The optimization result can be expressed by Eq. (1) [12-13];

$$q_{predicted} = a + \sum_{i=A}^{C} b_i i + \sum_{i=A}^{C} c_{ii} i^2 + \sum_{i=A}^{C} \sum_{j=A}^{C} d_{ij} ij \quad (1)$$

where $q_{predicted}$ (mg/L) is the predicted value of response; i and j are the independent parameters (A, B, and C) in the form of coded value; a, b_i, c_{ii}, and d_{ij} are the equation, linear, quadratic, and two-way interactions constants, respectively.

Crystal violet dye removal

The removal capacity of crystal violet on MIL-100(Fe) was obtained by batch adsorption for every MIL-100(Fe) produced from combined fabrication parameters. Here, 10 mg of MIL-100(Fe) was added into 10 mL of aqueous crystal violet solution with a 1000 mg/L concentration. Then, the mixture was shaken in a shaker water bath at room temperature for 24 h. After that, the supernatant was separated using a centrifuge, and its concentration was measured using a Shimadzu UV/Vis spectrophotometer at 590 nm of maximum wavelength. The removal capacity of crystal violet on MIL-100(Fe) (q) was calculated by the Eq. (2) [12-13];

$$q = \frac{(C_i - C_f)V}{m} \quad (2)$$

where c_i and C_f are the concentration of aqueous crystal violet solution at the initial and final conditions, V is the initial volume of the aqueous crystal violet solution, and m is the initial mass of MIL-100(Fe).

■ RESULTS AND DISCUSSION

Effects of Parameters on Fabricated MIL-100(Fe)

The OFAT method has been conducted to investigate the effects of ligand-to-metal molar ratio, fabrication time, and acetic acid concentration on the ability of MIL-100(Fe) to remove crystal violet dye from its aqueous solution. The removal capacity of crystal violet on MIL-100(Fe) is used as the response to determine the effects of these three independent parameters. Fig. 1 shows the OFAT design experiment and its results showing changes in removal capacity with increasing levels of each parameter. First, the OFAT experiments began by varying the ligand-to-metal molar ratio (0.50, 0.75, 1.00, and 1.25) at a constant fabrication time (4.0 h) and acetic acid concentration (5.0 vol%). Fig. 1(a) shows that the highest removal capacity was found at a ligand-to-metal molar ratio of 1.00. At low ligand-to-metal molar ratio, a lack of ligand in the formation of MIL-100(Fe) results in undersized solids and excessive metal residue. In this case, undersized solids have a lower surface area so their removal capacity increases along with the ligand-to-metal molar ratio. On the other hand, the use of a high ligand-to-metal molar ratio also leaves excess ligand residue so that the effect will reach a peak at a certain point as shown in Fig. 1(a). Here, this ligand residue tends to easily remain on the surface and pores of MIL-100(Fe), thereby reducing the

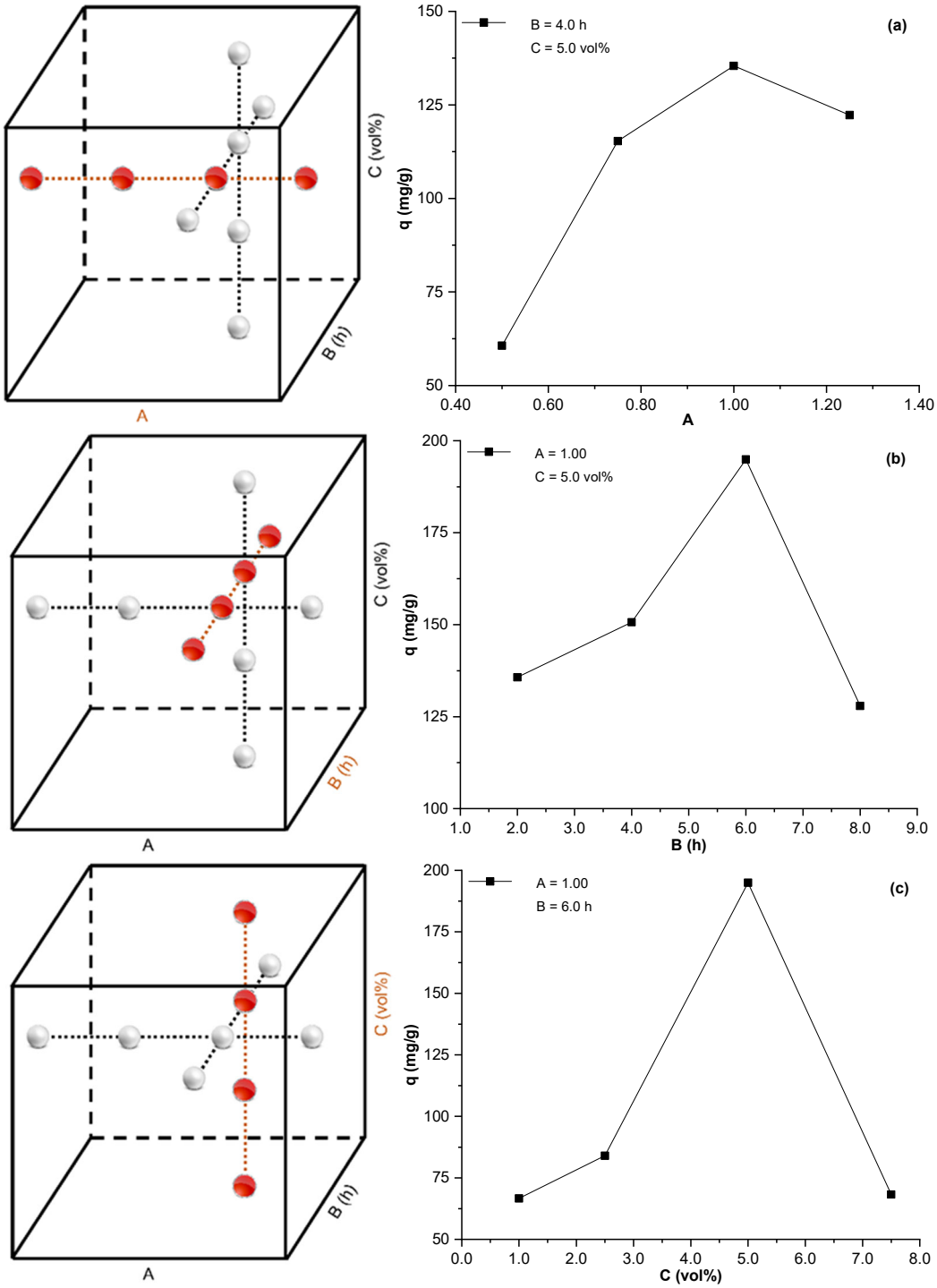

Fig 1. The effects of (a) ligand-to-metal molar ratio, (b) fabrication time, and (c) acetic acid concentration on MIL-100(Fe) based on the OFAT study

adsorption active site of MIL-100(Fe).

Second, the OFAT study was continued by varying the fabrication time (2.0, 4.0, 6.0, and 8.0 h) at a constant ligand-to-metal molar ratio (1.00) and acetic acid concentration (5.0 vol%). Here, MIL-100(Fe) can be fabricated efficiently in 6.0 h according to the OFAT results shown in Fig. 1(b). In general, the growth in size and expansion of surface area will occur along with the

fabrication time, which will affect the removal capacity of crystal violet on MIL-100(Fe). However, the formation of MIL-100(Fe) becomes saturated after a certain time, so the MIL-100(Fe) solids tend to agglomerate and lower their removal capacity. Third, the effects of varying acetic acid concentration (1.0, 2.5, 5.0, and 7.5 vol%) at constant ligand-to-metal molar ratio (1.00) and fabrication time (6.0 h) were also studied with the same OFAT method. Fig. 1(c) shows that the highest removal capacity of crystal violet on MIL-100(Fe) reached 194.94 mg/g when using an acetic acid concentration of 5.0 vol%. In this fabrication, acetic acid plays an important role in controlling the coordination bonds formed in the formation of MIL-100(Fe) where the nucleation rate is very sensitive to pH conditions. The presence of acetic acid in the system creates competitive reactions between Fe ions with acetic acid as monocarboxylic acid and H_3BTC as tricarboxylic acid. At a certain concentration, this competition effectively controls the formation of MIL-100(Fe) nuclei and avoids the phenomenon of intergrown structure.

Fabrication of MIL-100(Fe) and Its Statistical Studies

In the RSM study, 60 experimental runs were conducted using the CCD model, and the experimental values of the response were generated, as shown in Table 3. RSM analysis was conducted based on these data to investigate the statistical analysis of three independent parameters used. The statistical study generates a mathematical correlation between three independent parameters and their interactions on the removal capacity of crystal violet as the response expressed by the polynomial equation, as described in Eq. (3);

$$q_{predicted} = 192.25 - 6.83A + 4.58B + 2.68C - 17.59A^2 - 28.87B^2 - 49.15C^2 + 3.22AB - 0.64AC - 1.66BC \quad (3)$$

where $q_{predicted}$ (mg/g) is the predicted removal capacity of crystal violet on MIL-100(Fe) based on this mathematical correlation; A, B, and C are three independent parameters in the form of their coded value. In Table 3, the experimental and predicted responses show similar values with relatively low errors.

Table 3. The experimental and predicted responses for each combined parameter based on the RSM study

Run order	Blocks	Points	Parameters			Responses (mg/g)	
			A	B (h)	C (vol%)	$q_{experimental}$	$q_{predicted}$
1	1	Cube	−1	−1	−1	97.86	97.83
2			+1	−1	−1	61.03	79.01
3			−1	+1	−1	98.59	103.87
4			+1	+1	−1	95.33	97.93
5			−1	−1	+1	109.51	107.79
6			+1	−1	+1	86.85	86.41
7			−1	+1	+1	107.50	107.19
8			+1	+1	+1	105.69	98.69
9		Axial	−1.68	0	0	153.19	154.68
10			+1.68	0	0	125.76	131.71
11			0	−1.68	0	108.14	103.59
12			0	+1.68	0	99.33	119.00
13			0	0	−1.68	42.00	49.43
14			0	0	+1.68	59.36	58.44
15		Center	0	0	0	197.00	192.95
16			0	0	0	200.13	192.95
17			0	0	0	194.56	192.95
18			0	0	0	182.84	192.95
19			0	0	0	188.16	192.95
20			0	0	0	192.62	192.95

Run order	Blocks	Points	Parameters			Responses (mg/g)	
			A	B (h)	C (vol%)	$q_{experimental}$	$q_{predicted}$
21	2	Cube	−1	−1	−1	104.76	97.83
22			+1	−1	−1	74.14	79.01
23			−1	+1	−1	105.64	103.87
24			+1	+1	−1	105.34	97.93
25			−1	−1	+1	111.32	107.79
26			+1	−1	+1	90.28	86.41
27			−1	+1	+1	123.58	107.19
28			+1	+1	+1	95.37	98.69
29		Axial	−1.68	0	0	142.95	154.68
30			+1.68	0	0	147.51	131.71
31			0	−1.68	0	110.38	103.59
32			0	+1.68	0	117.02	119.00
33			0	0	−1.68	52.85	49.43
34			0	0	+1.68	62.39	58.44
35		Center	0	0	0	189.81	192.95
36			0	0	0	196.71	192.95
37			0	0	0	186.56	192.95
38			0	0	0	193.47	192.95
39			0	0	0	179.14	192.95
40			0	0	0	196.22	192.95
41	3	Cube	−1	−1	−1	106.67	97.83
42			+1	−1	−1	86.74	79.01
43			−1	+1	−1	117.36	103.87
44			+1	+1	−1	103.98	97.93
45			−1	−1	+1	99.82	107.79
46			+1	−1	+1	80.20	86.41
47			−1	+1	+1	113.74	107.19
48			+1	+1	+1	87.34	98.69
49		Axial	−1.68	0	0	144.35	154.68
50			+1.68	0	0	134.17	131.71
51			0	−1.68	0	98.57	103.59
52			0	+1.68	0	123.03	119.00
53			0	0	−1.68	44.58	49.43
54			0	0	+1.68	51.11	58.44
55		Center	0	0	0	197.95	192.95
56			0	0	0	189.76	192.95
57			0	0	0	209.19	192.95
58			0	0	0	190.29	192.95
59			0	0	0	204.29	192.95
60			0	0	0	186.43	192.95

Therefore, it can be stated that the CCD model used fits well with the statistical simulation carried out on this MIL-100(Fe) fabrication. Besides that, it is also proven by high R^2, R^2(adj), and R^2(pred) values at 97.57, 97.02, and 96.11%, respectively. Furthermore, the surface plots are used to illustrate the correlations between the

combination of two parameters at one constant parameter on the removal capacity of crystal violet on MIL-100(Fe) as shown in Fig. 2.

Along with the RSM analysis, ANOVA results were also presented in the statistical study as shown in Table 4. The linear, quadratic, and two-way interaction effects are evaluated for significance on the response where the *p*-values must be less than 0.05. Here, only the two-way interaction between parameters gives insignificant effects on the fabrication of MIL-100(Fe). The reliability of these ANOVA results is proven by the *p*-value of lack-of-fit (> 0.05), which indicates that the model error does

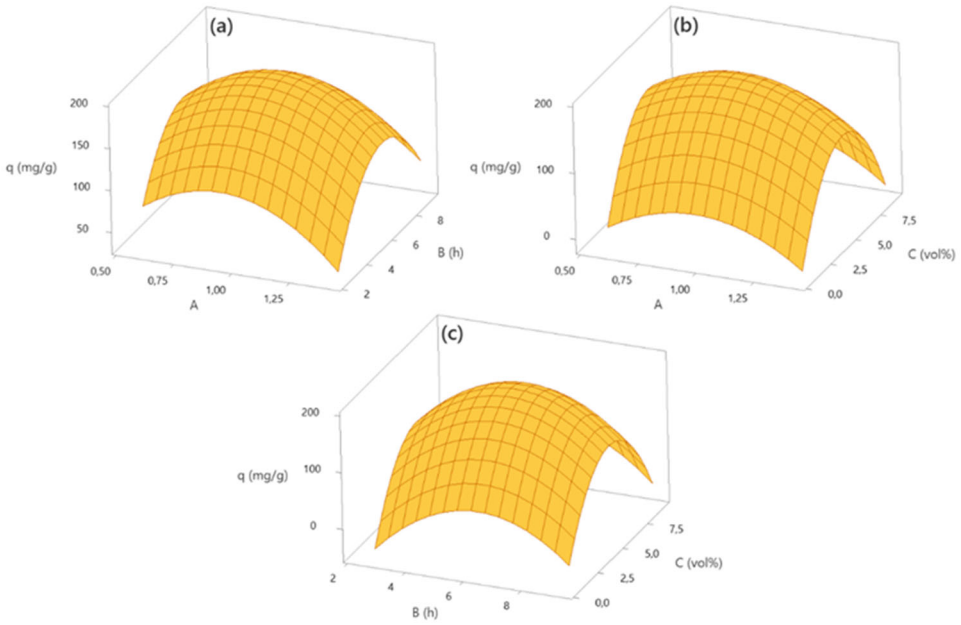

Fig 2. The surface plots of the effects between parameters: (a) A and B at C = 5.0 vol%, (b) A and C at B = 6.0 h, and (c) B and C at A = 1.00

Table 4. The ANOVA results of MIL-100(Fe) fabrication

Sources	DF	Sum of squares	Mean squares	*F*-value	*p*-value	Remarks
Model	11	138010	12546	175.34	0.000	Significant
Linear effects						
A	1	1909	1909	26.68	0.000	Significant
B	1	861	861	12.03	0.001	Significant
C	1	295	295	4.13	0.048	Significant
Quadratic effects						
A^2	1	13370	13370	186.85	0.000	Significant
B^2	1	36024	36024	503.46	0.000	Significant
C^2	1	104431	104431	1459.48	0.000	Significant
Two-way interaction effects						
AB	1	249	249	3.49	0.068	Not significant
AC	1	10	10	0.14	0.712	Not significant
BC	1	66	66	0.92	0.342	Not significant
Error	48	3435	72			
Lack-of-Fit	33	2606	79	1.43	0.233	Not significant
Pure error	15	829	55			
Total	59	141445				

not affect the overall statistical results. Moreover, Fig. 3 also shows the feasibility of these statistical studies where the normal probability plot, residuals-versus-fits plot, histogram, and residuals-versus-order plot provide normal results without any indication of irrelevancy.

Optimization and Validation Studies of MIL-100(Fe) Fabrication

The fabrication of MIL-100(Fe) was optimized based on the statistical data above to obtain the optimum condition for these three independent parameters. In the previous study, the adsorption capacity of rhodamine B on MIL-100(Fe) reached < 100 mg/g [7], so the optimization target in this study was set at 200 mg/g, twice as high as in the previous study. Fig. 4 shows the result of the optimization study where optimum MIL-100(Fe) can be fabricated using a ligand-to-metal molar ratio of 0.95 and an acetic acid concentration of 5.1 vol% for 6.2 h. This result indicates that the optimum removal capacity can reach 193.78 mg/g with a composite desirability of 0.9606, which means 96.06% of the target is achieved. Here, the validation was carried out to prove the optimization results which were done in three replicated runs as shown in Table 5. The optimization is satisfactory based on the validation, which shows a low error percentage (5.74 ± 1.97%) between the optimum and experimental removal capacity of crystal violet on MIL-100(Fe). In addition, the removal capacity of crystal violet on MIL-100(Fe) (193.78 mg/g) is higher than other adsorbents investigated from previous studies, such as

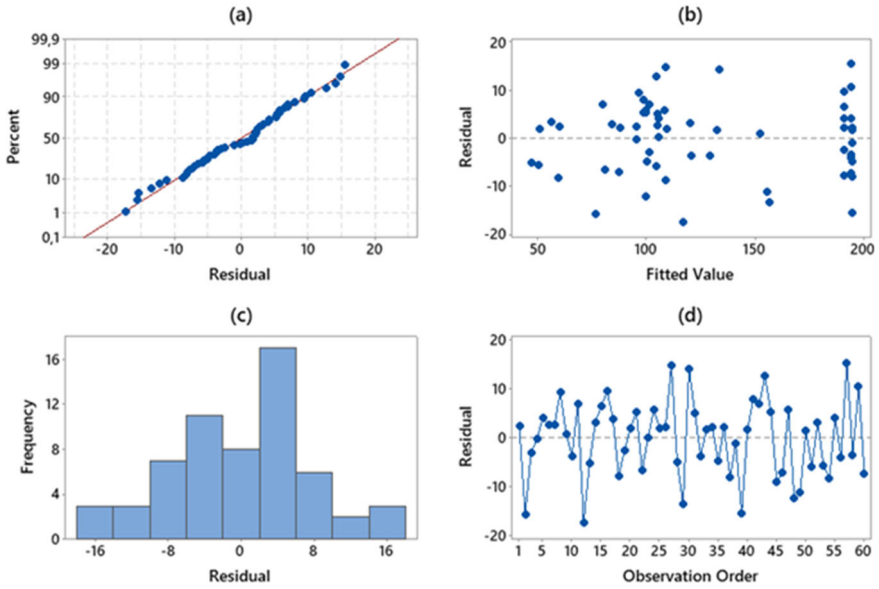

Fig 3. The feasibility of an RSM study for MIL-100(Fe) fabrication based on (a) normal probability plot, (b) residuals-versus-fits plot, (c) histogram, and (d) residuals-versus-order plot

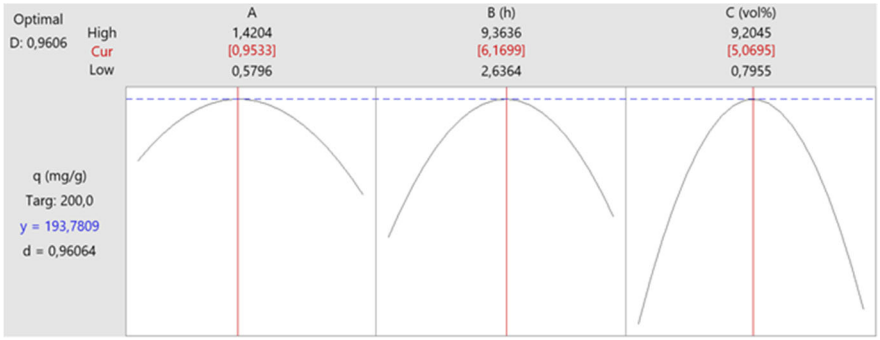

Fig 4. The optimization results of three independent parameters on MIL-100(Fe) fabrication

Table 5. The validation of MIL-100(Fe) fabrication at its optimum condition

Runs	Parameters			$q_{experimental}$ (mg/g)
	A	B (h)	C (vol%)	
1				179.09
2	0.95	6.2	5.1	186.68
3				182.20
Mean $q_{experimental}$ (mg/g)				182.66 ± 3.81
$q_{optimum}$ (mg/g)				193.78
Mean error (%)				5.74 ± 1.97

charred rice husk (62.85 mg/g), xanthated rice husk (90.02 mg/g) [14], and cross-linked chitosan-coated bentonite (169.49 mg/g) [15].

Characterizations of Fabricated MIL-100(Fe)

The optimum MIL-100(Fe) has been successfully created and optimized using a green method in terms of using room temperature and water/ethanol-based solvents. Fig. 5(a) shows the morphology of MIL-100(Fe), indicating nanosized particles with an average size of about 92.9 nm (using ImageJ software), which is in accordance with previous studies presenting the same morphology [16-18]. Here, the use of room-temperature conditions triggers the formation of nanosized MIL-100(Fe) due to its slow nucleation [17]. In the EDX analysis and mapping shown in Fig. 5(a) and 5(b), there are three main elements indicated in this material, such as carbon (49.86 wt.%), oxygen (45.11 wt.%), and iron (5.03 wt.%).

Based on the diffractogram of XRD shown in Fig. 6(a), there are several lattice planes indicating MIL-100(Fe), such as (333), (428), (088), (7911), (4814), (6618), and (9321), at 2θ values of 6.72°, 10.50°, 14.02°, 18.67°, 20.12°, 24.00°, and 27.67°, respectively. The presence and similarity of these lattice planes to previous studies prove that the fabricated MIL-100(Fe) has the same crystallinity [19-21]. The diffractogram pattern of MIL-100(Fe) is different from MIL-100(Fe) produced by conventional methods in previous studies [4,22-23]. In this diffractogram, wide peaks and several noise peaks indicate the amorphous characteristics of this MIL-100(Fe) produced by the green fabrication method at room temperature. Furthermore, the FTIR spectra shown in Fig. 6(b) exhibit that the functional groups of MIL-100(Fe) originate from its precursors (metal and ligand sources). The transmittance peaks at 474.5, 624.9, and 943.1 cm^{-1} indicate Fe–O stretching, Fe–O–Fe stretching, and Fe–O geometrical stretching of MIL-100(Fe) [19]. These functional groups denote the interactions between Fe cores and bridging ligands in the formation of MIL-100(Fe). Other specific peaks in the fingerprint region of the spectra are detected as C=C, C–H, C–O, O–H, and C=O stretching vibrations at 711.7, 758.0, 1116.7, 1380.9, 1446.5, and 1624.0 cm^{-1}, respectively [18-19]. The presence of bridging ligands in MIL-100(Fe) structures is indicated by the aromatic ring and tricarboxylic group stretching at 1571.9 and 1712.7 cm^{-1} [19-20]. In addition, the functional group of O–H stretching vibration from adsorbed water is shown in the peak at 3200–3600 cm^{-1} [17-20]. Eventually, the

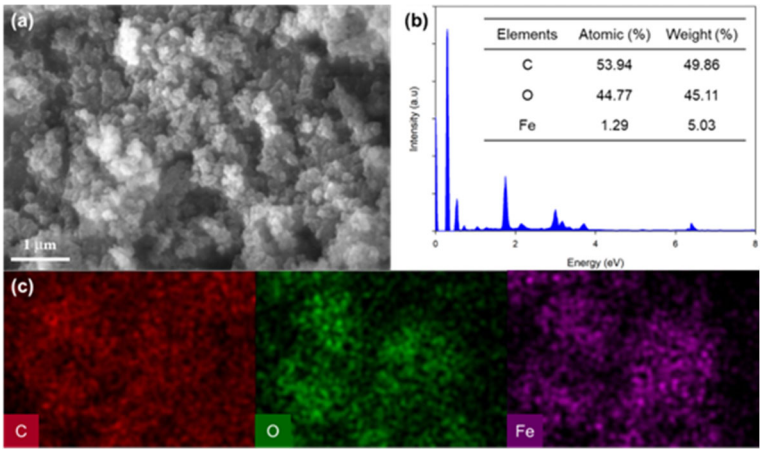

Fig 5. The morphology of MIL-100(Fe) based on (a) SEM image along with (b) EDX analysis and (c) EDX mapping

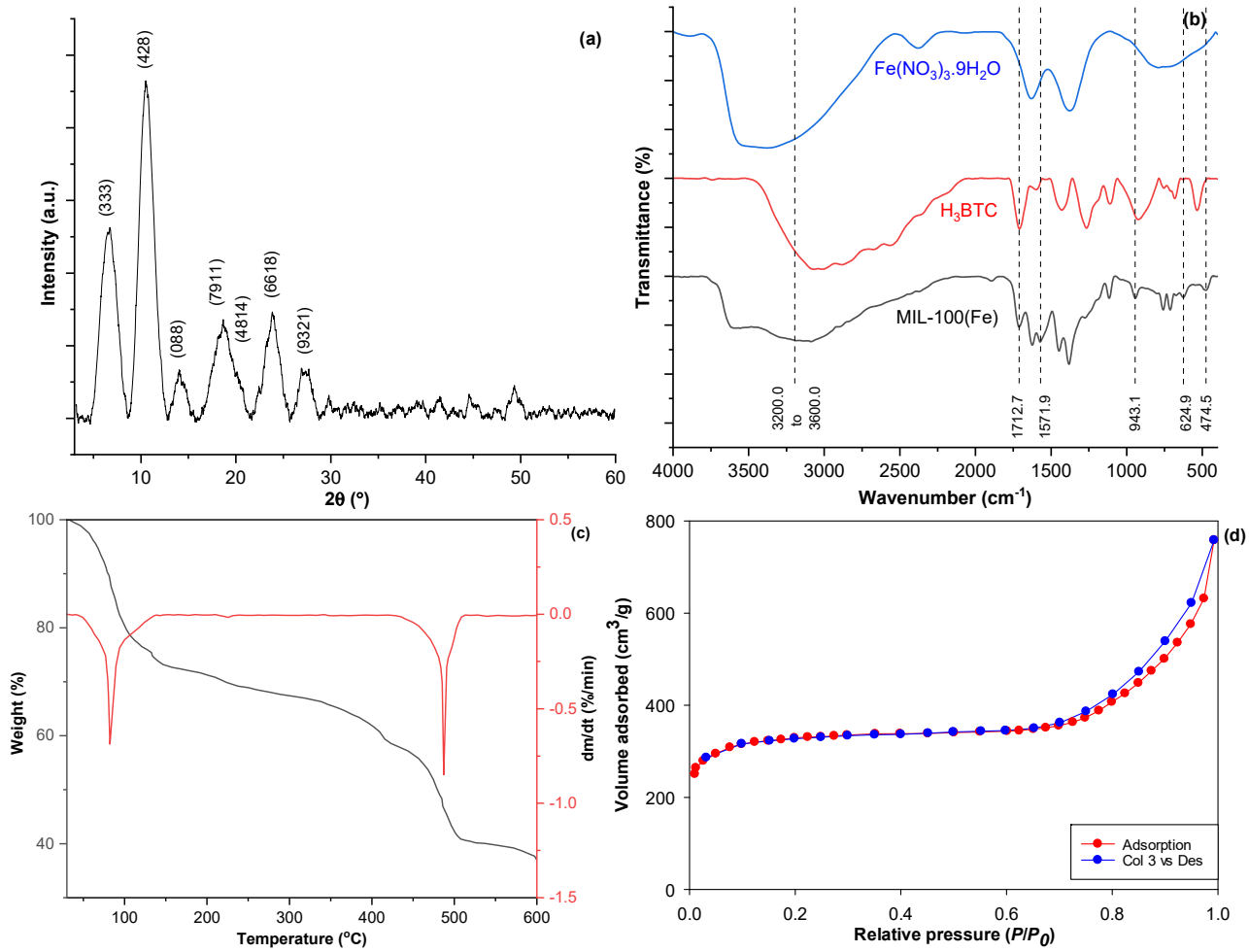

Fig 6. The MIL-100(Fe) characteristics based on (a) XRD, (b) FTIR, (c) TGA, and N_2 sorption analysis

thermal stability of MIL-100(Fe) is up to 450 °C based on the TGA/DTG spectra shown in Fig. 6(c). The TGA spectrum shows that there are at least two steps of weight loss, indicating moisture content loss at < 140 °C and decomposition of MIL-100(Fe) at 450–500 °C. Here, the MIL-100(Fe) structure begins to collapse at temperatures above 450 °C due to the degradation of bridging ligands [19,23]. In addition, the N_2 sorption analysis results from the surface area and pore volume of MIL-100(Fe) reaching 1210.08 m^2/g and 1.09 cm^3/g, respectively, based on the multiple-point Brunauer–Emmett–Teller (BET) measurement. Fig. 6(d) shows the N_2 adsorption-desorption isotherm curve of MIL-100(Fe) with type I and IV isotherms indicating the possession of micro- and mesopores [23-24]. The existence of a narrow hysteresis loop with a type H1 loop supports the presence of uniform mesopores [25].

■ CONCLUSION

In this study, MIL-100(Fe) has been successfully fabricated under an optimum condition from the statistical studies. An optimum and green fabrication method has been developed using water/ethanol-based solvents at room temperature. MIL-100(Fe) has good physical and chemical characteristics, making it very versatile for various applications. The optimum MIL-100(Fe) is a promising adsorbent for dye removal due to its high removal capacity, reaching 182.66 ± 3.81 mg/g. Further adsorption studies are still needed to investigate the interactions of MIL-100(Fe) in the adsorption system.

■ ACKNOWLEDGMENTS

The authors would like to acknowledge the financial support from the Directorate General of

Higher Education, Research and Technology of the Ministry of Education, Culture, Research, and Technology [Grant No. 268M/WM01.5/N/2023].

■ CONFLICT OF INTEREST

The authors declare no conflict of interest.

■ AUTHOR CONTRIBUTIONS

The conceptualization, methodology, supervision, project administration, funding acquisition, and resources were done by Christian Julius Wijaya, Felycia Edi Soetaredjo, Suryadi Ismadji, and Setiyo Gunawan. The software, validation, writing–original draft preparation, and review were done by Christian Julius Wijaya, Maria Yuliana, Shella Permatasari Santoso, Sandy Budi Hartono, and Wenny Irawaty. The sample analysis, investigation, data curation, and visualization were done by Christian Julius Wijaya, Jindrayani Nyoo Putro, Jenni Lie, Chintya Gunarto, and Nathania Puspitasari. All authors agreed to the final version of this manuscript.

■ REFERENCES

[1] Al-Tohamy, R., Ali, S.S., Li, F., Okasha, K.M., Mahmoud, Y.A.G., Elsamahy, T., Jiao, H., Fu, Y., and Sun, J., 2022, A critical review on the treatment of dye-containing wastewater: Ecotoxicological and health concerns of textile dyes and possible remediation approaches for environmental safety, *Ecotoxicol. Environ. Saf.*, 231, 113160.

[2] Rafaqat, S., Ali, N., Torres, C., and Rittmann, B., 2022, Recent progress in treatment of dyes wastewater using microbial-electro-Fenton technology, *RSC Adv.*, 12 (7), 17104–17137.

[3] Sriram, G., Bendre, A., Mariappan, E., Altalhi, T., Kigga, M., Ching, Y.C., Jung, H.Y., Bhaduri, B., and Kurkuri, M., 2022, Recent trends in the application of metal-organic frameworks (MOFs) for the removal of toxic dyes and their removal mechanism-A review, *Sustainable Mater. Technol.*, 31, e00378.

[4] Guesh, K., Caiuby, C.A.D., Mayoral, Á., Díaz-García, M., Díaz, I., and Sanchez-Sanchez, M., 2017, Sustainable preparation of MIL-100(Fe) and its photocatalytic behavior in the degradation of methyl orange in water, *Cryst. Growth Des.*, 17 (4), 1806–1813.

[5] Shindhal, T., Rakholiya, P., Varjani, S., Pandey, A., Ngo, H.H., Guo, W., Ng, H.Y., and Taherzadeh, M.J., 2021, A critical review on advances in the practices and perspectives for the treatment of dye industry wastewater, *Bioengineered*, 12 (1), 70–87.

[6] Zhang, W., Zhang, Y.Z., and Yang, J.M., 2022, MIL-100(Fe)@GO composites with superior adsorptive removal of cationic and anionic dyes from aqueous solutions, *J. Mol. Struct.*, 1265, 133365.

[7] Jang, H.Y., Kang, J.K., Park, J.A., Lee, S.C., and Kim, S.B., 2020, Metal-organic framework MIL-100(Fe) for dye removal in aqueous solutions: Prediction by artificial neural network and response surface methodology modeling, *Environ. Pollut.*, 267, 115583.

[8] Fang, Y., Yang, Z., Li, H., and Liu, X., 2020, MIL-100(Fe) and its derivatives: From synthesis to application for wastewater decontamination, *Environ. Sci. Pollut. Res.*, 27 (5), 4703–4724.

[9] Du, M., Xu, G., Zhang, J., Guan, Y., Guo, C., and Chen, Y., 2023, Hierarchically porous MIL-100(Fe) with large mesopores for cationic dye adsorption, *J. Solid State Chem.*, 322, 123950.

[10] Huang, C.W., Zhou, S.R., and Hsiao, W.C., 2024, Multifunctional TiO_2/MIL-100(Fe) to conduct adsorption, photocatalytic, and heterogeneous photo-Fenton reactions for removing organic dyes, *J. Taiwan Inst. Chem. Eng.*, 158, 104850.

[11] Gnanasekaran, G., Sudhakaran, M.S.P., Kulmatova, D., Han, J., Arthanareeswaran, G., Jwa, E., and Mok, Y.S., 2021, Efficient removal of anionic, cationic textile dyes and salt mixture using a novel CS/MIL-100(Fe) based nanofiltration membrane, *Chemosphere*, 284, 131244.

[12] Wijaya, C.J., Ismadji, S., Aparamarta, H.W., and Gunawan, S., 2021, Facile and green synthesis of starfruit-like ZIF-L, and its optimization study, *Molecules*, 26 (15), 4416.

[13] Wijaya, C.J., Ismadji, S., Aparamarta, H.W., and Gunawan, S., 2021, Statistically optimum HKUST-1

synthesized by room temperature coordination modulation method for the adsorption of crystal violet dye, *Molecules*, 26 (21), 6430.

[14] Homagai, P.L., Poudel, R., Poudel, S., and Bhattarai, A., 2022, Adsorption and removal of crystal violet dye from aqueous solution by modified rice husk, *Heliyon*, 8 (4), e09261.

[15] Vithalkar, S.H., and Jugade, R.M., 2020, Adsorptive removal of crystal violet from aqueous solution by cross-linked chitosan coated bentonite, *Mater. Today: Proc.*, 29, 1025–1032.

[16] Duan, S., Li, J., Liu, X., Wang, Y., Zeng, S., Shao, D., and Hayat, T., 2016, HF-free synthesis of nanoscale metal–organic framework NMIL-100(Fe) as an efficient dye adsorbent, *ACS Sustainable Chem. Eng.*, 4 (6), 3368–3378.

[17] Li, W., Zhang, T., Lv, L., Chen, Y., Tang, W., and Tang, S., 2021, Room-temperature synthesis of MIL-100(Fe) and its adsorption performance for fluoride removal from water, *Colloids Surf., A*, 624, 126791.

[18] Mahmoodi, N.M., Abdi, J., Oveisi, M., Alinia Asli, M., and Vossoughi, M., 2018, Metal-organic framework (MIL-100 (Fe)): Synthesis, detailed photocatalytic dye degradation ability in colored textile wastewater and recycling, *Mater. Res. Bull.*, 100, 357–366.

[19] Chaturvedi, G., Kaur, A., Umar, A., Khan, M.A., Algarni, H., and Kansal, S.K., 2020, Removal of fluoroquinolone drug, levofloxacin, from aqueous phase over iron based MOFs, MIL-100(Fe), *J. Solid State Chem.*, 281, 121029.

[20] He, W., Li, Z., Lv, S., Niu, M., Zhou, W., Li, J., Lu, R., Gao, H., Pan, C., and Zhang, S., 2021, Facile synthesis of Fe_3O_4@MIL-100(Fe) towards enhancing photo-Fenton like degradation of levofloxacin via a synergistic effect between Fe_3O_4 and MIL-100(Fe), *Chem. Eng. J.*, 409, 128274.

[21] Yuan, B., Wang, X., Zhou, X., Xiao, J., and Li, Z., 2019, Novel room-temperature synthesis of MIL-100(Fe) and its excellent adsorption performances for separation of light hydrocarbons, *Chem. Eng. J.*, 355, 679–686.

[22] Zhang, W., Shi, Y., Li, C., Zhao, Q., and Li, X., 2016, Synthesis of bimetallic MOFs MIL-100(Fe-Mn) as an efficient catalyst for selective catalytic reduction of NO_x with NH_3, *Catal. Lett.*, 146 (10), 1956–1964.

[23] Simon, M.A., Anggraeni, E., Soetaredjo, F.E., Santoso, S.P., Irawaty, W., Thanh, T.C., Hartono, S.B., Yuliana, M., and Ismadji, S., 2019, Hydrothermal synthesize of HF-free MIL-100(Fe) for isoniazid-drug delivery, *Sci. Rep.*, 9 (1), 16907.

[24] Sapnik, A.F., Ashling, C.W., Macreadie, L.K., Lee, S.J., Johnson, T., Telfer, S.G., and Bennett, T.D., 2021, Gas adsorption in the topologically disordered Fe-BTC framework, *J. Mater. Chem. A*, 9 (47), 27019–27027.

[25] Thommes, M., Kaneko, K., Neimark, A.V., Olivier, J.P., Rodriguez-Reinoso, F., Rouquerol, J., and Sing, K.S.W., 2015, Physisorption of gases, with special reference to the evaluation of surface area and pore size distribution (IUPAC Technical Report), *Pure Appl. Chem.*, 87 (9-10), 1051–1069.